Applied Chemical Engineering (2025) Volume 8 Issue 1 ISSN: 2578-2010 (O)
doi: 10.59429/ace.v8i1.5618

RESEARCH ARTICLE

Synthesis and application of SA-g-poly (AAc-IA)/ bentonite composite for norfloxacin drug adsorption from aqueous solution

Sajjad H. Irhayyim[1], **Layth S. Jasim**[2,*]

[1] *Ministry of Education, Directorate of Education Al-Qadisiyah, AL- Diwaniya, 61002, Iraq*

[2] *Department of Chemistry, College of Education, University of Al-Qadisiyah, Diwaniya, 61003, Iraq*

***Corresponding author:** Layth S. Jasim, layth.alhayder@qu.edu.iq

ABSTRACT

This research explored the creation and application of a composite material, SA-g-poly (AAc-IA)/bentonite, for removing Norfloxacin (NOR) from water. Synthesized through copolymerization, the composite's properties were characterized using FTIR, TGA, FESEM, and AFM. FTIR analysis confirmed essential functional groups, with shifts observed in the 1500–1750 cm^{-1} range post-NOR adsorption. FESEM images showed a porous surface, with particle sizes between 50–200 nm, that became less porous after adsorption. TGA analysis indicated thermal stability up to 300°C, followed by significant decomposition between 300–550°C due to organic component breakdown. Adsorption studies revealed equilibrium within 120 minutes, with a maximum adsorption capacity of 9.99 mg/g. Thermodynamic analysis confirmed a spontaneous and endothermic process, with ΔH of +23.76 kJ/mol. Kinetic modeling showed a pseudo-second-order mechanism, indicating chemisorption. These findings suggest the SA-g-poly (AAc-IA)/bentonite composite is a potentially efficient and cost-effective adsorbent for pharmaceutical wastewater treatment.

Keywords: Adsorption; hydrogel; composite; norfloxacin

ARTICLE INFO

Received: 17 February 2025
Accepted: 7 March 2025
Available online: 19 March 2025

1. Introduction

Norfloxacin (NOR) is a widely employed antibiotic that enters the environment by different pathways, as wastewater and improper disposal[1-3]. Its presence in water bodies, soil, and sediments may result in development of antibiotic-resistant bacteria, posing serious threats to aquatic life and human health[4,5]. Traditional water treatment methods often fail to completely remove NOR due to its antimicrobial properties. Given the significant environmental risks associated with NOR contamination, there is an urgent need for the development of effective and practical methods to eliminate this antibiotic from water sources[6,7]. Existing primary methods for the removal of water treatment include membrane separation[8,9], advanced oxidation processes[10,11], and photolysis[12-14]. However, these techniques often exhibit one or more significant limitations[15-17], including high operational costs, demanding reaction conditions, prolonged treatment durations, or the generation of harmful byproducts[15,18]. The surge in advancements within adsorbent materials has significantly increased the appeal of adsorption process[19,20]. This is primarily due to their user-friendly operation[21], high treatment effectiveness, cost-effectiveness, and environmentally friendly nature[22].

Till date, numerous materials like hydrogel spheres, polymeric materials, nano-materials, clay minerals and biochar based materials have been used for NOR adsorption[23]. Bentonite, a cost-effective clay mineral, offers high adsorption potential due to its cation exchange capacity and layered silicate structure. However, its limited functional groups and separation challenges restrict its use. Modifications, like interlayer cation introduction, enhance its surface area and reactivity, improving contaminant removal. To address separation issues, granulation is employed. Sodium alginate (along with other polymeric materials), a non-toxic biopolymer, serves as a binder for bentonite encapsulation, creating easily separable composite beads. This combination, particularly with organically modified bentonite, effectively removes contaminants like NOR from wastewater, balancing adsorption efficiency with practical application[24,25].

Zhou and Sun enhanced NOR adsorption by modifying bentonite with surfactants and sodium alginate granulation. This created a rough, layered composite with improved porosity. Adsorption was endothermic, favored acidic conditions, and was enhanced by cations. Dynamic column tests showed breakthrough time varied with bed height, flow rate, and pH, fitting Thomas and Yoon–Nelson models, indicating diffusion was not rate-limiting[25]. Gopal and Mukherjee investigated the use of chitosan-coated Fe-Cu nanocomposite alginate-CMC beads (NBs) to remove Norfloxacin (NOR) from water. Under optimal conditions, they achieved 86% NOR removal. The beads exhibited a Langmuir adsorption capacity of 355 mg g^{-1}, attributed to multiple adsorption mechanisms. They also found that the beads effectively reduced the toxicity of NOR solutions to algae. The study concluded that these nanocomposite beads are a promising wastewater treatment material due to their ease of synthesis, high adsorption capacity, stability, and environmental friendliness[26]. However, this study involved the use of sodium alginate-grafted-poly (acrylic acid-Itaconic acid, (SA-g-poly (AAc-IA))/ bentonite composite for adsorptive removal of NOR from water. Hydrogels are 3D networks of hydrophilic polymers that exhibit significant water absorption and retention capabilities. These materials function effectively as sorbents due to their high swelling capacity and the presence of active sites within their structure that can capture dyes. The incorporation of bentonite clay into polymer hydrogels enhances their adsorption properties by increasing the overall surface area and porosity. Furthermore, the interactions between the clay and the hydrogel network contribute to improved mechanical strength of resulting material[27,28]. The composite was synthesized by the method of copolymerization and characterized with FTIR, TGA, FESEM and AFM techniques. Effect of time and temperature on NOR adsorption was also explored and data from these studies was applied to kinetic and thermodynamic model, respectively for better understanding of the adsorption mechanism.

2. Materials and methods

2.1. Chemicals and materials

Sodium alginate (Macline, China), acrylic acid (AAc) (Himedia, India), persulfate potassium (KPS) (Fluka, Germany), Itaconic acid (IA) (Macline, China), N, N'-methylene bisacrylamide (MBA) (Fluka, Germany) and Norfloxacin, **Figure 1,** (Macline, China). All of the reagents were of analytical grade and used without any further purification. All solutions were prepared with deionized water to ensure that they were free of contaminants.

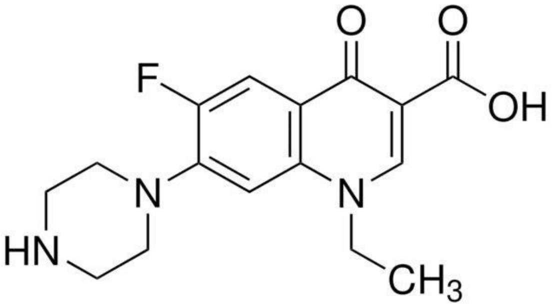

Figure 1. Structure of Norfloxacin (NOR) drug.

2.2. Preparation of SA-g-poly (AAc-IA)/ bentonite composite

The polymeric composite, SA-g-poly (AAc-IA)/ bentonite (**Figure 2**), was prepared by copolymerization method in several steps. Firstly, 0.5 g sodium alginate was dissolved in 17 mL distilled water by stirring for an hour at a temperature of 30 °C. Afterwards, 5 mL acrylic acid was added to above solution followed by mixing with itaconic acid solution (0.5 g in 5 ml water). In next step, KPS solution (0.05 g in 2 ml distilled water) was added followed by mixing mixture with cross-linking agent, MBA, (0.05 g in 2 ml distilled water). Afterwards, 5 ml bentonite with a concentration of 100 ppm (0.5 g in 50 ml of water) was added in the presence of nitrogen gas to form free radicals. After the time of 180 min (maintained at temperature of 70 °C in a water bath), the polymerization process occurs resulting in the formation of composite that was then taken out, cut to small pieces and washed several times to remove any unreacted materials. The prepared composite was characterized by Fourier Transform Infrared Spectroscopy (FTIR), Thermal Gravimetric Analysis (TGA), Field Emission Scanning Electron Microscopy (FESEM) and Atomic Force microscopy (AFM).

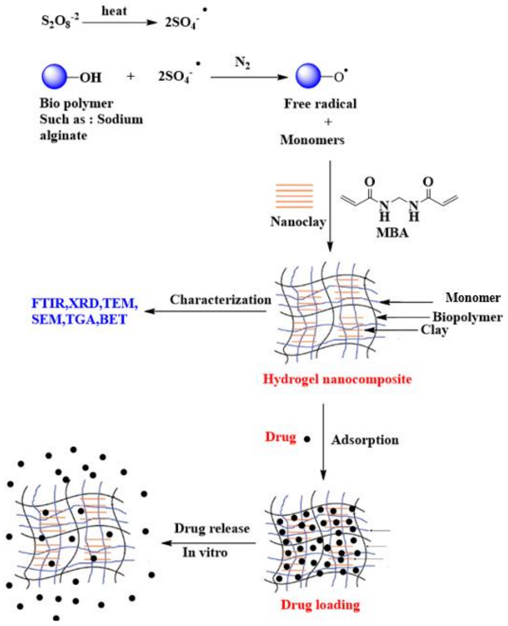

Figure 2. Synthesis of SA-g-poly (AAc-IA)/ bentonite composite.

3. Results and discussion

3.1. Calibration curve of NOR

The calibration curve for norfloxacin was determined using diluted concentrations ranging from (1-17 ppm) at 276 nm and the results of the calibration curve are shown in **Figure 3.** The coefficient of determination

(R^2) for curve is 0.9995, indicating a very strong linear relationship between NOR concentration and absorbance. This high R^2 value suggests that the calibration curve is reliable for determining the concentration of NOR in samples within the measured concentration range.

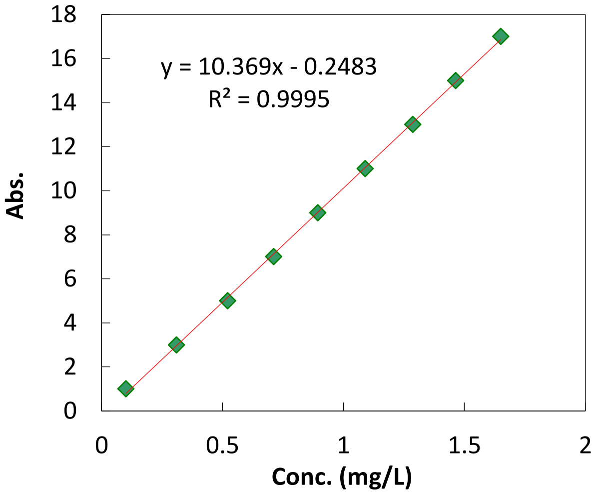

Figure 3. Calibration curve of NOR.

3.2. Characterization results

The surface of composite SA-g-poly (AAc-IA)/ bentonite was studied using FTIR technology before and after the adsorption of drug (NOR) (**Figure 4).** The analysis of composite before drug adsorption shows the appearance of a broad and wide band at 3050 cm^{-1} to 3400 cm^{-1}. This is due to the presence of active -OH groups in sodium alginate and bentonite. The band in range 2750 cm^{-1} to 2920 cm^{-1} refers to aliphatic C-H group, which causes extensible vibrations. The band in range 1680 cm^{-1} to 1550 cm^{-1} refers to C=O group. For carboxylic acid, which is present in composition of IA and AAc, the range 1090 cm^{-1} to 1450 cm^{-1} corresponds to presence of C-C, C-O, and C-N groups. After adsorption of drug (NOR), bands in between 1500 cm^{-1} to 1700 cm^{-1} corresponds to presence of large number of aromatic C=C groups. When nanoparticles were introduced, the FTIR spectrum showed alterations between 1500 and 1750 cm^{-1}, pointing to a reaction between the composite and Norfloxacin. The alterations, specifically changes in the C=O and C=C peaks, signify that Norfloxacin successfully bonded to the composite. This suggests that strong chemical forces, like hydrogen bonding and electrostatic interactions, facilitated the binding. The changes in peak placement and strength validate that the adsorption process altered the composite's structure[25,29-32].

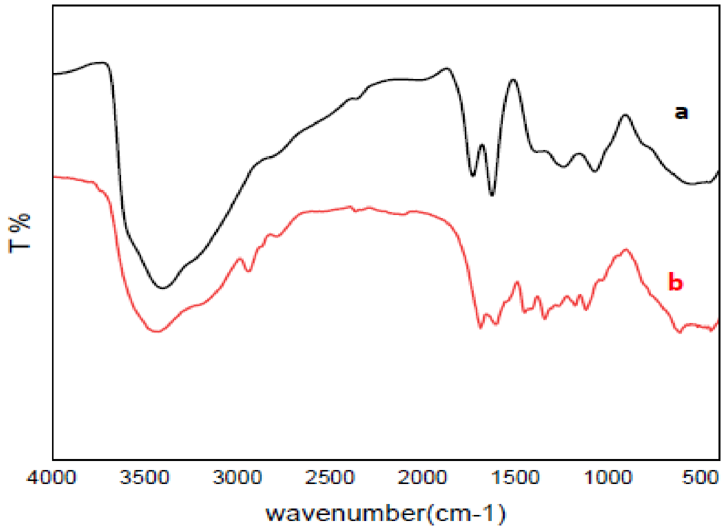

Figure 4. FTIR analysis for SA-g-poly (AAc-IA)/ bentonite (a) before and (b) after NOR adsorption.

The FESEM technique was used to study the surface properties of prepared composite i.e., SA-g-poly (AAc-IA)/ bentonite before and after NOR adsorption. This analysis aid in understanding the crystal structure, surface size, shape of particles, and nature of their aggregates among themselves, in addition to knowing the nature of surface (either porous or smooth). FESEM images of compound before adsorption, shown in **Figure 5a,** showed that it has a porous structure with a rough surface in form of irregular aggregates that are heterogeneous in size and shape. The reason for this is the presence of active functional groups as hydroxyl and carboxyl groups[33]. After adsorption of drug molecules on surface of composite SA-g-poly (AAc-IA/ bentonite), **Figure 5b,** the surface of composite became less porous and somewhat homogeneous. This could be attributed to adsorption of drug molecules on composite surface[34,35].

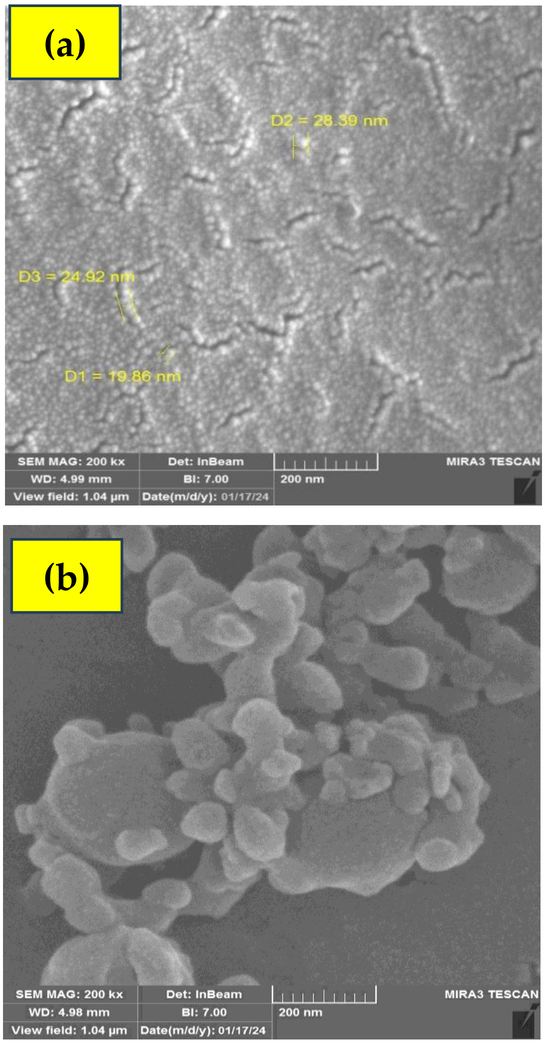

Figure 5. FESEM of SA-g-poly (AAc-IA)/ bentonite composite (a) before and (b) after drug adsorption.

The thermal behavior of prepared composite SA-g-poly (AAc-IA)/ bentonite was studied using TGA/ DTA technique, where the samples were heated in presence of nitrogen gas within a temperature range of 40 °C to 900 °C at a rate of 10min/ °C. Results of TGA curve (**Figure 6**) showed that prepared composite, SA-g-poly (AAc-IA)/ bentonite), undergo weight loss that takes place in four stages. The first stage was due to loss of water molecules adsorbed on composite surface, second and third stages were due to loss of functional groups containing oxygen as hydroxyl, carboxyl, and epoxy. The last stage was due to the thermal decomposition of cross-linked polymer chains. In summary, the TGA results show that between 300 and 550°C, the composite lost weight due to the breakdown of organic functional groups. Further heating, past 550°C, caused the polymer network to decompose, leaving mostly bentonite. At 750°C, the remaining ash, primarily bentonite, likely has minimal to no adsorption capacity due to the loss of the polymer structure. The disintegration of polymer network, and DTA curve help in getting knowledge about the presence of water molecules within the gel structure, as confirmed by presence of a band within the range located between 100 °C to 300 °C. Additionally, it helps in determining the type of reaction as if the direction of beam is upward then this indicates that the reaction is an emitter (-) while on the other hand, if the direction of beam is downward, this indicates that the reaction is an absorber (+)[36]. **Figure (6)** and **Table 1** explains the results of thermogravimetric decomposition[12,37,38].

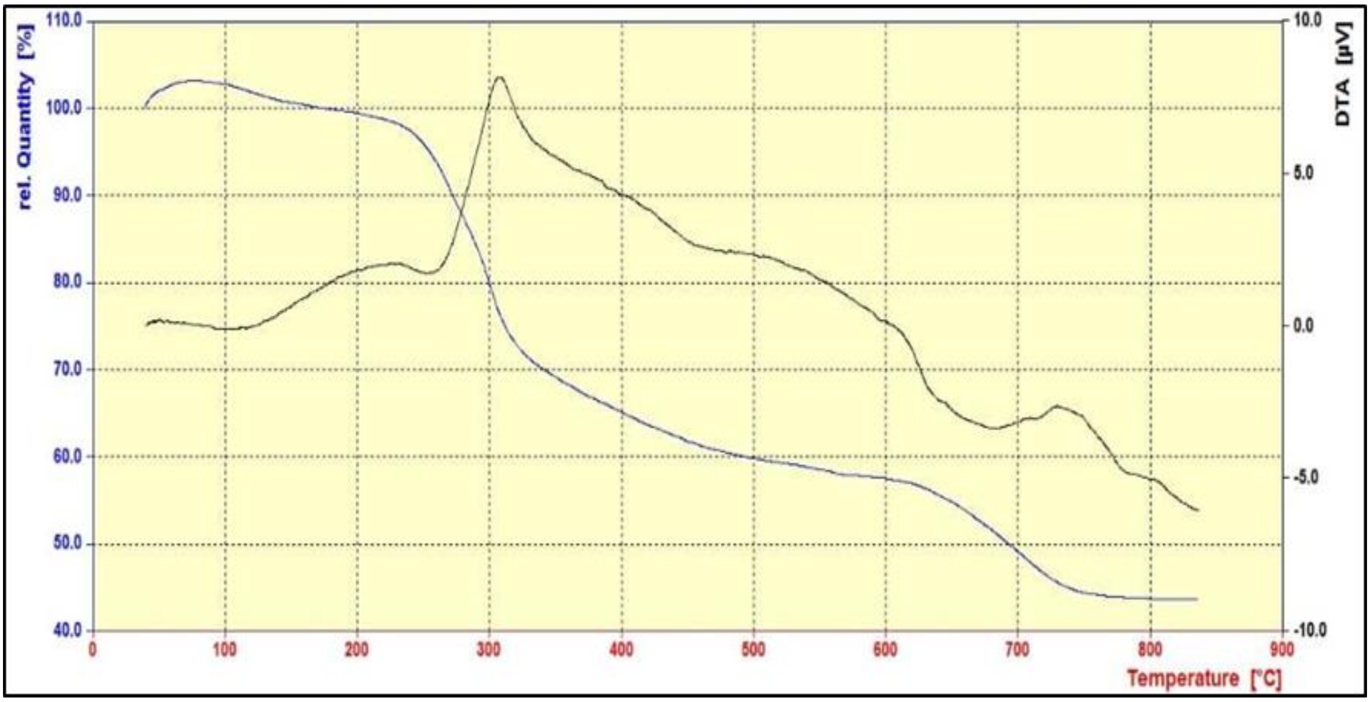

Figure 6. TGA curve of P(AA-co-1-MeCPAI) hydrogels.

Table 1. Thermogravimetric decomposition values of composite, SA-g-poly (AAc-IA)/ bentonite.

Step	TG Rang C°	Mass loos%	DTA(DSC)
1	25-247	3.95	215(+)
2	247-335	24.61	305(+)
3	335-546	18.12	597(-)
4	546-751	11.7	737(-)

Using an atomic force microscope, statistical information about the topography of prepared SA-g-poly (AAc-IA)/ bentonite composite and values of distribution ranges, homogeneity, thickness, and surface roughness based on the Root Mean Square Roughness (RMS) can be determined (**Figure 7** showing three-dimensional image of overlaid hydrogel). **Table 2** shows the most important statistical values for surface roughness of composite. It is also evident from the negative value of surface torsion R_{sk} that the distribution of dips on surface is greater than peaks. If the value of surface torsion R_{sk} is positive, this indicates that the distribution of peaks is greater than the dips in surface, while if value of R_{sk} is equal to zero then this means that distribution of heights and depressions on composite surface is similar. It was observed through the surface flatness value R_{ku} of prepared composite that it has a bumpy surface ($R_{ku} > 3$)[39,40].

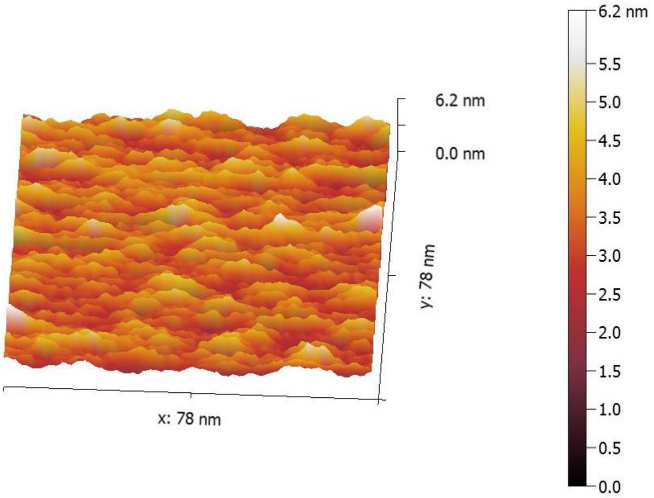

Figure 7. A 3D AFM image of prepared SA-g-poly (AAc-IA)/ bentonite composite.

Table 2. Statistical roughness coefficients for surface of SA-g-poly (AAc-IA)/ bentonite composite.

Statistical value of roughness	SA-g-poly (AAc-IA)/ bentonite
Roughness rate, nm (R_a)	2.382
Root mean square roughness, nm (R_q)	3.419
Surface warping, nm (R_{sk})	-1.581
Leveling of peaks, nm (R_{ku})	11.04
The upper limit of height of the peaks, nm (R_p)	12.08
Minimum depth of roughness, nm (R_v)	22.57
Maximum height of rough surface, nm (R_z)	34.66

3.3. Thermal study

The adsorption of norfloxacin on surface of the composite was studied at different temperatures (288, 293, 298, 303) K, and the results showed that the adsorption increases with increasing temperatures as shown in **Figure 8** and **Table 3.** Results of the study revealed that adsorption process is endothermic as an increase in temperature leads to an increase in the movement of particles due to an increase in kinetic energy resulting from breaking the bond forces between them. This led to an increase in rate of spread of adsorbed fine particles on composite surface layer. Furthermore, adsorbent surface porosity and pore size also increase with increasing temperature[25,41]. The linear relationship, as well as value of change in enthalpy (ΔH) for adsorption of drug molecules on surface of SA-g-poly (AAc-IA)/ bentonite composite was obtained by plotting the reciprocal of absolute temperature (1/T) versus ln X_m), as shown in **Figure 9** and the **Table 4.**

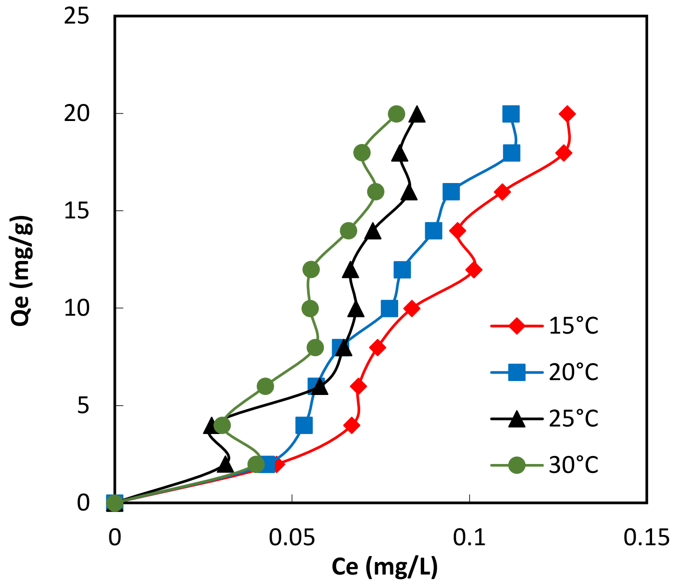

Figure 8. Adsorption of NOR on surface of SA-g-poly (AAc-IA)/ bentonite composite at different temperatures.

Table 3. Adsorption of NOR on surface of SA-g-poly (AAc-IA)/ bentonite composite at different temperatures.

15 °C		**20 °C**		**25 °C**		**30 °C**	
C_e (mg/L)	**Q_e (mg/g)**	**C_e (mg/L)**	**Q_e (mg/g)**	**C_e (mg/L)**	**Q_e (mg/g)**	**C_e (mg/L)**	**Q_e (mg/g)**
0.045646	1.990871	0.042752	1.99145	0.031179	1.993764	0.039859	1.992028
0.066863	3.986627	0.053361	3.989328	0.027322	3.994536	0.030312	3.993938
0.068695	5.986261	0.056833	5.988633	0.057797	5.988441	0.042463	5.991507
0.074096	7.985181	0.06368	7.987264	0.064548	7.98709	0.056544	7.988691
0.08374	9.983252	0.077471	9.984506	0.06802	9.986396	0.055097	9.988981
0.101292	11.97974	0.08104	11.98379	0.066477	11.9867	0.055386	11.98892
0.096663	13.98067	0.089912	13.98202	0.072746	13.98545	0.065898	13.98682
0.109297	15.97814	0.094831	15.98103	0.082968	15.98341	0.073614	15.98528
0.126656	17.97467	0.111901	17.97762	0.080365	17.98393	0.069756	17.98605

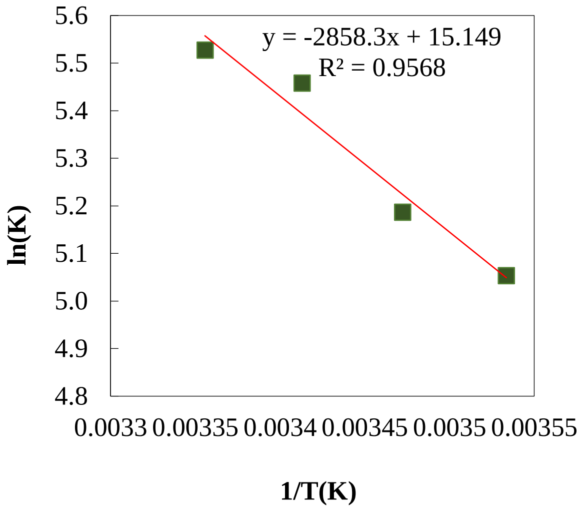

Figure 9. Plot of ln X_m against reciprocal absolute temperature for adsorption of NOR.

Table 4. Effect of temperature on maximum adsorbed quantity of NOR.

T (°C)	T (K)	1000/ T (K^{-1})	NOR	
			C_e =46.5	
			X_m	ln X_m
15	288	0.00353	156.5	**5.053147217**
20	293	0.00347	178.8	**5.186481739**
25	298	0.00341	234.6	**5.457791015**
30	303	0.00336	251.4	**5.526978319**

The thermodynamic functions for adsorption process of drug molecules on surface of prepared composite were calculated as shown in **Table 5**, as Gibb's free energy change (ΔG) is a negative value, which means that the adsorption process occurred automatically. The change in entropy of system (ΔS) is a positive value showing that the degrees of freedom of drug molecules are high and mobile[35]. Additionally, the value of enthalpy change (ΔH) is positive revealing that the adsorption is an endothermic process i.e., by increasing temperature, the adsorption will increase[42-44].

Table 5. Values of thermodynamic functions of adsorption process of NOR at 25 °C.

ΔH (kJ. mol^{-1})	ΔG (kJ. mol^{-1})	ΔS (J. K^{-1}.mol^{-1})	Equilibrium constant (K)
23.764	-13.693	125.949	251.383

3.4. Kinetic study

Practical experiments have shown that the time required to reach equilibrium was 120 minutes as shown in the **Figure 10.** In the beginning, the adsorption process was more effective. Given that the active sites are ready for adsorption, and with the passage of time, the amount of adsorbed material has reached a state of equilibrium and stability. After an equilibrium, the adsorption process begins to slow down because of filing of maximum active sites of composite[45].

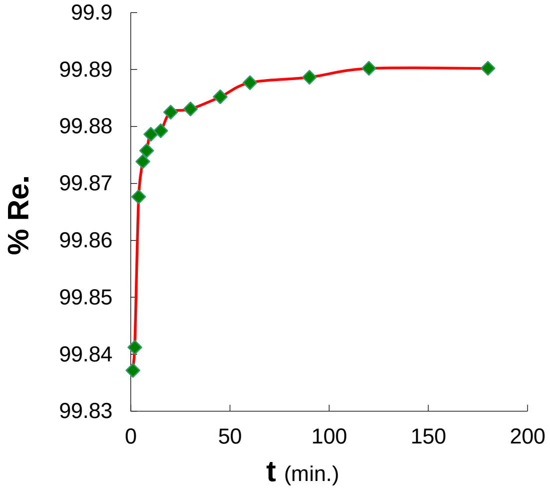

Figure 10. Effect of reaction time on NOR adsorption.

Kinetic models i.e., pseudo-first-order (Equation 1) and pseudo-second-order (Equation 2) models were applied on time study data, as illustrated in **Figure 11.**

$$\log(Q_e - Q_t) = \log Q_e - \frac{k_1}{2.303} t \tag{4}$$

$$\frac{t}{Q_t} = \frac{1}{k_2 Q_e^2} + \frac{t}{Q_e} \tag{5}$$

here Q_t (mg/g), Q_e (mg/g) refers to amount of adsorbed dye after time t (min) and at equilibrium, correspondingly. k_1 (1/min) and k_2 (g/mg·min) denotes rate constant for pseudo-first as well as second model correspondingly[46]. Correlation coefficients and kinetic constants were also calculated for both models. The results showed that value of correlation coefficient (R^2) for pseudo-second-order model is 1 (**Table 6**). This means that pseudo-second-order model is more suitable for describing kinetics compared to the pseudo-first-order model[47-49].

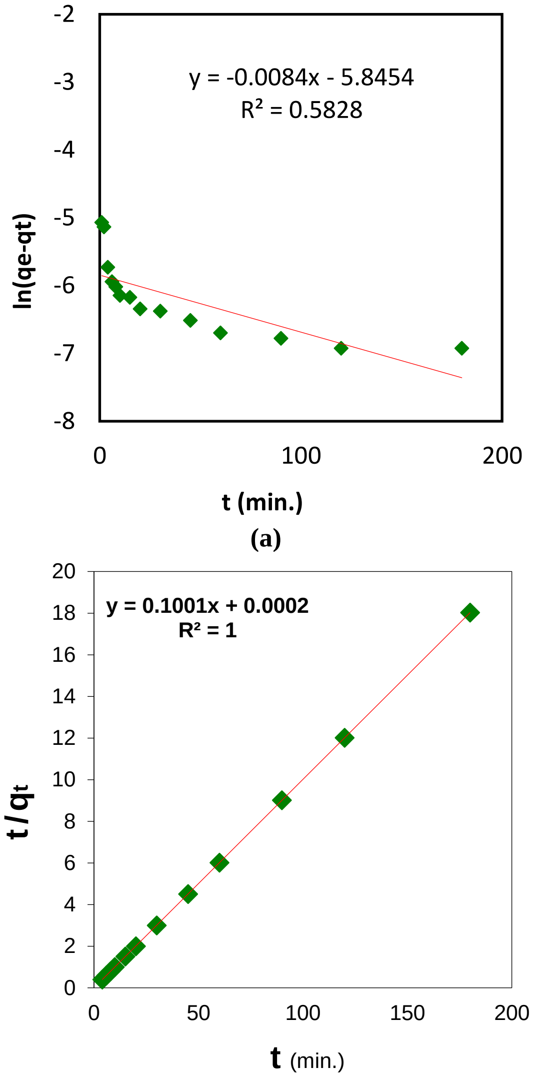

(a)

(b)

Figure 11. Kinetic models for adsorption of NOR drug (A) pseudo-first order and (B) pseudo-second order.

Table 6. Kinetic constants for pseudo-first and pseudo-second models for NOR drug adsorption on composite.

Adsorbate	**Pseudo-first order**				
	R^2	**Q_e (mg/g)**	**K_1 (min^{-1})**	**Intercept**	**Slope**
R6G	0.5828	0.002893	0.0084	-5.8454	-0.0084

Adsorbate	**Pseudo-second order**					
	h ($mg.g^{-1}.min^{-1}$)	**R^2**	**Q_e (mg/g)**	**K_2 ($g.mg^{-1}.min^{-1}$)**	**Intercept**	**Slope**
R6G	5000	1	9.99001	50.10005	2.00E-04	0.1001

4. Conclusion, limitations and future outlook

The presence of pharmaceutical byproducts, especially antibiotics like Norfloxacin, in water sources creates serious ecological and health concerns, largely due to the rise of antibiotic-resistant strains. Traditional water purification methods struggle to fully eliminate these pollutants. To address this, a new composite material, combining sodium alginate, acrylic acid, itaconic acid, and bentonite, was created to improve the removal of Norfloxacin from contaminated water. The composite's characteristics, including its porous structure, key functional groups, and thermal stability, were thoroughly analyzed using various techniques. Experiments revealed that Norfloxacin was effectively removed from water, with the process being energetically favorable. The adsorption followed a chemical reaction-driven pattern, indicating strong bonding between the Norfloxacin and the composite. This research introduces a potentially affordable and environmentally friendly adsorbent for treating pharmaceutical-laden wastewater. The composite's ease of production, biocompatibility, and potential for scaling up make it a promising candidate for real-world applications. Future research should concentrate on increasing its capacity to adsorb pollutants, improving its ability to target a variety of contaminants, and developing methods to reuse the material. Furthermore, incorporating this composite into more advanced water treatment systems could lead to more sustainable solutions for reducing pharmaceutical pollution.

While the composite demonstrated promising Norfloxacin removal, its practical application faces several hurdles. The adsorption capacity, though notable, may be inadequate for industrial-scale wastewater treatment, necessitating further research to optimize surface area and functional group density. Moreover, its selectivity in complex environmental matrices, containing diverse contaminants beyond Norfloxacin, requires thorough investigation. The absence of desorption and regeneration studies hinders assessment of its long-term economic viability and reusability. Future research should prioritize developing cost-effective regeneration processes and evaluating the composite's performance under varying environmental conditions. A more detailed kinetic and diffusion analysis is also crucial to optimize process parameters and address potential mass transfer limitations. Furthermore, scaling up the laboratory synthesis for practical applications demands attention to composite stability, environmental impact, and modifications to polymerization conditions. Future studies should also focus on exploring alternative modification methods to enhance adsorption performance and broaden the composite's applicability to a wider range of contaminants. Ultimately, addressing these limitations and focusing on these future directions will be essential for translating the composite's promising laboratory results into effective and sustainable wastewater treatment solutions.

Author contributions

Authors contributed equally to the manuscript.

Acknowledgments

Authors would like to acknowledge University of Al-Qadisiyah for administrative and technical support.

Conflict of interest

The authors declare no conflict of interest

References

1. Khan, N.A., et al., Occurrence, sources and conventional treatment techniques for various antibiotics present in hospital wastewaters: a critical review. TrAC Trends in Analytical Chemistry, 2020. 129: p. 115921.
2. Aminnezhad, S., et al., Revolutionizing medicine: Molecularly imprinted polymers as precision tools in cancer diagnosis and antibiotic detection. Cellular and Molecular Biology, 2024. 70(5): p. 100-110.

3. Abdulsahib, W.K., et al., Adsorption Study of Cephalexin Monohydrate Drug in Solution on Poly (vinyl pyrrolidone-acryl amide) Hydrogel Surface. International Journal of Drug Delivery Technology, 2021. 11(4): p. 1169-1172.
4. Yuan, X., et al., Occurrence, fate, and mass balance of selected pharmaceutical and personal care products (PPCPs) in an urbanized river. Environmental Pollution, 2020. 266: p. 115340.
5. Cobian-Solorio, G., et al., Non-steroidal anti-inflammatory drugs adsorption from aqueous solution by MOFs MIL-100 (Fe), ZIF-8 and UiO-66: Synthesis, characterization, and comparative study. Journal of Molecular Structure, 2025. 1321: p. 139698.
6. Kulik, K., A. Lenart-Boroń, and K. Wyrzykowska, Impact of antibiotic pollution on the bacterial population within surface water with special focus on mountain rivers. Water, 2023. 15(5): p. 975.
7. Radhy, N.D. and L.S. Jasim, A novel economical friendly treatment approach: Composite hydrogels. Caspian Journal of Environmental Sciences, 2021. 19(5): p. 841-852.
8. Shah, A., et al., Sequential novel use of Moringa oleifera Lam., biochar, and sand to remove turbidity, E. coli, and heavy metals from drinking water. Cleaner Water, 2024: p. 100050.
9. Shah, A., et al., A review of physicochemical and biological contaminants in drinking water and their impacts on human health. Water Science and Engineering, 2023.
10. Rehman, H., et al., Potential of easily available low-cost raw cotton for the elimination of methylene blue dye from polluted water. Desalination and Water Treatment, 2024. 318: p. 100319.
11. Zeeshan, M., et al., Investigating the Interactions between Dyes and Porous/Composite Materials: A Comprehensive Study. Sustainable Chemistry for the Environment, 2025: p. 100217.
12. Jamel, H.O., et al., Adsorption of Rhodamine B dye from solution using 3-((1-(4-((1H-benzo[d]imidazol-2-yl)amino)phenyl)ethylidene)amino)phenol (BIAPEHB)/ P(AA-co-AM) composite. Desalination and Water Treatment, 2025: p. 101019.
13. Majeed, H.J., et al., Synthesis and application of novel sodium carboxy methyl cellulose-g-poly acrylic acid carbon dots hydrogel nanocomposite (NaCMC-g-PAAc/CDs) for adsorptive removal of malachite green dye. Desalination and Water Treatment, 2024: p. 100822.
14. N. Zghair, A., et al., Synthesis, characterization and adsorption properties of azo-functionalized polymeric hydrogels for R6G dye removal from water. Applied Chemical Engineering, 2025. 8(1): p. ACE-5604.
15. Arshad, R., T. Javed, and A. Thumma, Exploring the efficiency of sodium alginate beads and Cedrus deodara sawdust for adsorptive removal of crystal violet dye. Journal of Dispersion Science and Technology, 2023: p. 1-14.
16. Javed, T., et al., Batch adsorption study of Congo Red dye using unmodified Azadirachta indica leaves: isotherms and kinetics. Water Practice & Technology, 2024: p. wpt2024020.
17. Rehman, H., et al., Potential of easily available low-cost raw cotton for the elimination of methylene blue dye from polluted water. Desalination and Water Treatment, 2024: p. 100319.
18. Xu, Z., et al., Enhancing drug solubility through competitive adsorption on silica nanosurfaces with ultrahigh silanol densities. Proceedings of the National Academy of Sciences, 2025. 122(4): p. e2423426122.
19. Hasan, R.C., F.F. Karam, and S.J. Baqir. Synthesis and characterization of a novel organic reagent and its complexes with Cu (||), Cr(|||), Co(|||) and Fe(|||) metal. in IOP Conference Series: Earth and Environmental Science. 2022.
20. Kmal, R.Q., et al., Removal of Toxic Congo Red Dye from Aqueous Solution Using a Graphene Oxide/Poly (Acrylamide-Acrylic acid) Hydrogel: Characterization, Kinetics and Thermodynamics Studies. Journal of Chemical Health Risks, 2022. 12(4): p. 609-619.
21. Shah, A., et al., The effect of dose, settling time, shelf life, storage temperature and extractant on Moringa oleifera Lam. protein coagulation efficiency. Environmental Nanotechnology, Monitoring & Management, 2024. 21: p. 100919.
22. Shah, A., et al., Removal of cadmium and zinc from water using Sewage sludge-derived biochar. Sustainable Chemistry for the Environment, 2024: p. 100118.
23. Zou, M., et al., Effective adsorption of norfloxacin from water on magnetic biochar composite derived from cellulase hydrolysis apple branch: Synthesis optimization, performance assessment and mechanism insight. Process Safety and Environmental Protection, 2024. 185: p. 435-444.
24. Ashrul Asbollah, M., et al., Individual and competitive adsorption of negatively charged acid blue 25 and acid red 1 onto raw Indonesian kaolin clay. Arabian Journal for Science and Engineering, 2022. 47(5): p. 6617-6630.
25. Zhou, J. and Q. Sun, Sodium alginate/modified bentonite composite bead adsorptive removal of norfloxacin: static and dynamic adsorption. Polymers, 2022. 14(19): p. 3984.
26. Gopal, G. and A. Mukherjee, Adsorptive removal of norfloxacin from aqueous solutions by Fe/Cu CNS-embedded alginate–carboxymethyl cellulose–chitosan beads. RSC advances, 2024. 14(23): p. 15862-15875.
27. Shah, L.A., et al., Bentonite clay reinforced alginate grafted composite hydrogel with remarkable sorptive performance toward removal of methylene green. International Journal of Biological Macromolecules, 2024. 279: p. 135600.

28. Rafak, S.H. and L.S. Jasim, Synthesis of novel bentonite/pectin-grafted-poly (crotonic acid-co-acrylic acid) hydrogel nanocomposite for adsorptive removal of safranin O dye from aqueous solution. International Journal of Environmental Analytical Chemistry, 2024: p. 1-24.
29. Batool, M., et al., Applications of biodegradable polymers and ceramics for bone regeneration: a mini-review. International Journal of Polymeric Materials and Polymeric Biomaterials: p. 1-15.
30. Batool, M., M.N. Haider, and T. Javed, Applications of Spectroscopic Techniques for Characterization of Polymer Nanocomposite: A Review. Journal of Inorganic and Organometallic Polymers and Materials, 2022. 32(12): p. 4478-4503.
31. Haider, M.N., M. Batool, and T. Javeed, Biodegradable Magnesium Metal for Bone Regeneration: Mini Review. International Journal of Medical Reviews, 2022. 9(1): p. 241-243.
32. Maged, A., et al., Characterization of activated bentonite clay mineral and the mechanisms underlying its sorption for ciprofloxacin from aqueous solution. Environmental Science and Pollution Research, 2020. 27: p. 32980-32997.
33. Salama, A., et al., Crosslinked alginate/silica/zinc oxide nanocomposite: a sustainable material with antibacterial properties. Composites Communications, 2018. 7: p. 7-11.
34. Ikhtiyarova, G., et al., Characterization of natural-and organobentonite by XRD, SEM, FT-IR and thermal analysis techniques and its adsorption behaviour in aqueous solutions. Clay Minerals, 2012. 47(1): p. 31-44.
35. Shah, A., et al., Adsorptive removal of arsenic from drinking water using KOH-modified sewage sludge-derived biochar. Cleaner Water, 2024: p. 100022.
36. Sarkar, M., et al., Polypropylene-clay composite prepared from Indian bentonite. Bulletin of Materials Science, 2008. 31: p. 23-28.
37. Park, J.-H., et al., Application of montmorillonite in bentonite as a pharmaceutical excipient in drug delivery systems. Journal of Pharmaceutical Investigation, 2016. 46: p. 363-375.
38. Shah, L.A., et al., Characterization of Pakistani purified bentonite suitable for possible pharmaceutical application. Applied Clay Science, 2013. 83: p. 50-55.
39. Yeo, J.Y.J., et al., Experimental and modelling study of adsorption isotherms of amoxicillin, ampicillin and doripenem on bentonite-chitosan composite. South African Journal of Chemical Engineering, 2023. 43(1): p. 38-45.
40. Kgabi, D.P. and A.A. Ambushe, Characterization of South African Bentonite and Kaolin Clays. Sustainability, 2023. 15(17): p. 12679.
41. Feng, D., et al., Adsorption characteristics of norfloxacin by biochar prepared by cassava dreg: kinetics, isotherms, and thermodynamic analysis. BioResources, 2015. 10(4): p. 6751-6768.
42. Ahmed, M.J., Adsorption of non-steroidal anti-inflammatory drugs from aqueous solution using activated carbons. Journal of environmental management, 2017. 190: p. 274-282.
43. Hassan, S. and J. Ibrahim, Adsorption of some drugs onto surface of Iraqi kaolin clay. Pak. J. Chem, 2011. 1(3): p. 132-137.
44. Fang, X., et al., High-efficiency adsorption of norfloxacin using octahedral UIO-66-NH2 nanomaterials: Dynamics, thermodynamics, and mechanisms. Applied Surface Science, 2020. 518: p. 146226.
45. Salihi, E.Ç. and M. Mahramanlıoğlu, Equilibrium and kinetic adsorption of drugs on bentonite: Presence of surface active agents effect. Applied Clay Science, 2014. 101: p. 381-389.
46. Saruchi, et al., Microwave synthesize karaya Gum-Cu, Ni nanoparticles based bionanocomposite as an adsorbent for malachite green dye: kinetics and thermodynamics. Frontiers in Materials, 2022. 9: p. 827314.
47. Dekhyl, B.K.M.A.B. and T.A.H.A.M. Abbas, Kinetic Study of Adsorption for Doxycycline Drug from Aqueous Solutions by Bentonite and Activation Bentonite at Different Temperatures.
48. Parashar, A., S. Sikarwar, and R. Jain, Studies on adsorption kinetics of norfloxacin using nano alumina in aqueous medium. Analytical Chemistry Letters, 2020. 10(2): p. 227-239.
49. Parab, H., et al., Use of agro-industrial wastes for removal of basic dyes from aqueous solutions. CLEAN–Soil, Air, Water, 2009. 37(12): p. 963-969.